

A Bidirectional DC-DC Converter—Analysis and Control Design

FELIX A HIMMELSTOSS, JOHANN W KOLAR AND FRANZ C ZACH

Power Electronics Section, Technical University of Vienna, Gusshausstrasse 27-29, A-1040 Vienna, Austria

A system for DC-DC power conversion based on a buck-boost converter topology is presented which makes power flow in both directions possible. The possibility of bidirectional power flow is useful for certain applications, such as uninterruptible power supplies (UPS) etc. The structure is compared with the well known unidirectional buck-boost converter. Open-loop control is treated based on simulation using duty cycle averaging. The system behaviour of the bidirectional converter is analyzed; a structure diagram is given and the transfer function of the system is derived. The validity of the duty cycle averaging is proven by comparison to a switched model. The controller for the converter is then realized as simple voltage controller, as voltage controller with an inner-loop current controller (cascade control) and with two kinds of state space control. The transfer functions of the different system parts are derived and dimensioning guide-lines for the controller sections are presented. The closed-loop behaviours of the bidirectional converter for the different control structures are analyzed based on simulation using duty cycle averaging; Bode diagrams and step responses are shown for an example. Finally, applications of the analyzed system are discussed.

Indexing terms : Bidirectional DC-DC power converter, Buck boost converter

UNIDIRECTIONAL converters in their basic configuration are characterized by an asymmetrical structure regarding their topology and/or regarding their controllability. Switching instants and conduction intervals of the diodes on the secondary are - dependent on the converter topology (buck or boost converters etc) - determined indirectly by changing the switching status of the power transistor on the primary.

An intrinsic limitation of this concept is given by the direction of current and energy flow (first quadrant of the current-voltage phase plane) which is determined by the direction of the electric valves.

Bidirectional power flow between constant voltage (current) sources requires replacement of the unidirectional power semiconductor devices by an antiparallel combination of a directly (power transistor) and an indirectly (diode) controllable electrical valve. This results in a unidirectionally controllable power semiconductor. However, this requires fixed voltage polarity, equivalent to restriction to the first and second quadrant of the current-voltage plane.

The application of this general concept to a buck-boost converter structure leads to a topology with a remarkably simple topology.

There is only one magnetic device necessary; (Fig 1) where this topology is compared to that of the conventional unidirectional buck-boost converter.

The stationary system condition is characterized by a

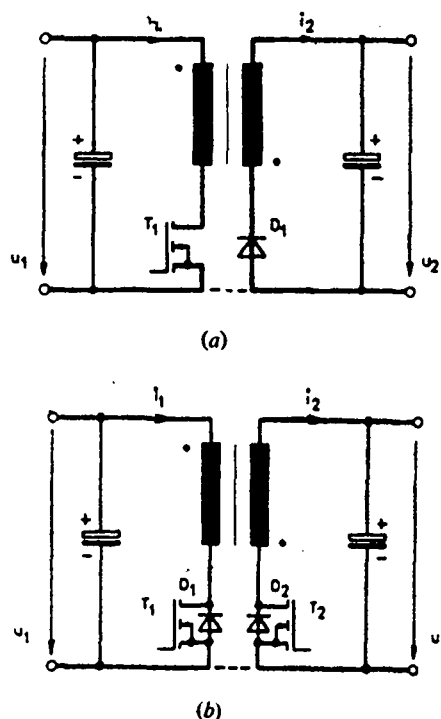


Fig 1 (a) Unidirectional buck-boost converter, (b) Bidirectional buck-boost converter

time constant average energy content of the primary and secondary electrical and magnetic energy storage devices.

This equilibrium between energy input and output corresponds to a duty ratio defined only by the voltage ratios (and turn ratios) of primary and secondary independent of the energy flow direction. This is shown in the following. Idealized components and push-pull control of T_1 and T_2 as indicated in Fig 2 are assumed. Vice

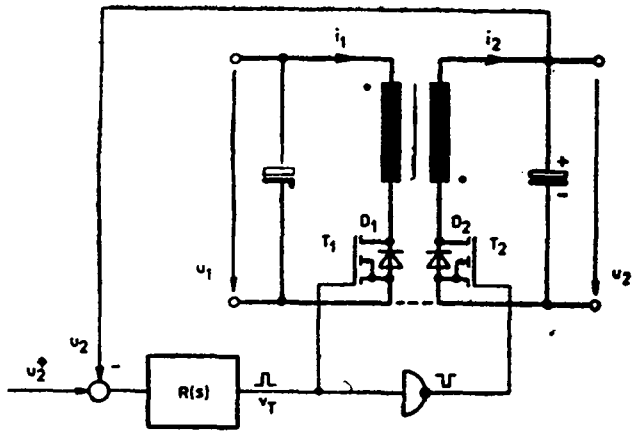


Fig 2 Bidirectional converter with push-pull control

versa by adjusting a duty ratio (for stationary, *ie* equilibrium operation) the voltage ratio of the converter can be varied to a large extent.

SYSTEM DESCRIPTION AND COMPARISON OF UNIDIRECTIONAL AND BIDIRECTIONAL BUCK BOOST CONVERTER

Continuous operation is given if the transistor on the primary is turned on again before i_{D_1} reaches zero (Fig 3).

If one considers a practical realization of the circuit with FETs one has to note that T_2 (T_1) conducts part of the current besides D_2 (D_1); this is due to the gate signal (push-pull control) being present also for positive i_2 (negative i_1); the current distribution corresponds to the parallel circuit of turn-on resistance and nonlinear diode characteristic.

Concerning efficiency of the described system one has to note critically that, as mentioned, for no (low) load condition the energy oscillates between input and output. This leads to a considerable deterioration of the efficiency in connection with the nonideal behaviour of the system components. The resistive losses appearing thereby can be reduced by reduction of the current ripple (increase of the effective inductances, increased size and volume, stray inductances). Further losses are due to magnetizing and demagnetizing the transformer core with switching frequency. The losses are largely load independent. However, this appears for each turn-off as energy converted into heat being proportional to the sum of the stray inductances and the square of the current ripple maximum. Therefore, one also has to consider that the blocking voltage across the semiconductor switch is formed by the sum of the supply voltage plus the transformed secondary voltage plus the voltage across the stray inductance.

MODEL REPRESENTATION OF THE BIDIRECTIONAL CONVERTER

For the derivation of the model equations for the bidirectional converter compare also [1,2].

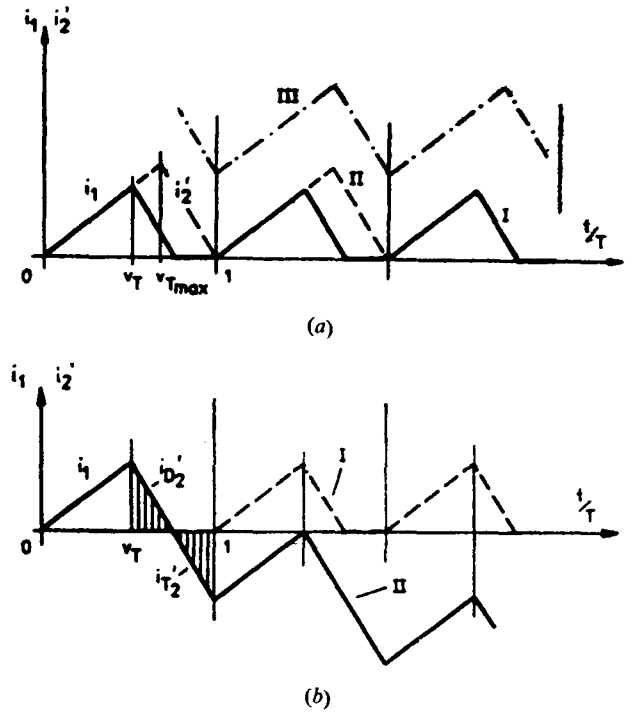


Fig 3 (a) Unidirectional converter (I) discontinuous current, (II) intermediate case, (III) continuous current, (b) Bidirectional converter (I) discontinuous current (usually not used for bidirectional operation), (II) continuous current

Parasitic elements considered are the (ohmic) resistances on the primary and secondary R_1, R_2 (consisting of the sums of the winding resistances and the R_{DSon} of the semiconductor switches).

For different load cases (ohmic load, current or voltage sources, loads with constant power consumption - all for the primary and/or secondary side) one can establish two describing differential equation systems for closed switch and for open switch on the primary. These two systems can be combined into one system of differential equations if one assumes switching periods small compared to the system time constants. Then the system of non-linear differential equations is linearized around its operating point.

As an example we consider the results for the U-R operation, *ie* where a voltage source is on the primary side and an ohmic load is on the secondary side. A closer investigation shows that the basic form of the transfer function (but, of course, not the coefficients) is equal for ohmic loads, for loads with constant current consumption and for loads with constant power consumption. This is also independent whether the load is on the primary or on the secondary side. The form of the transfer function between duty cycle and converter output voltage (or input voltage) is given by

$$G_{u\alpha}(s) = \frac{s \cdot z_{1u} + z_{0u}}{s^2 + s \cdot n_{1u} + n_{0u}} \tag{1}$$

Downloaded by [ETH Zurich] at 01:53 30 June 2015

For coupling of two rigid DC voltage systems we receive a simpler transfer function for the relationship between duty cycle and converter current of the following form

$$G_{ix}(s) = \frac{z_{0i}}{s + n_{0i}} \quad (2)$$

There n_{0i} is determined by the parasitic system resistances. Because n_{0i} is usually small, this means that the system basically forms an integrator.

During the interval t_{on} the equivalent circuit of Fig 4a is valid, leading to the equations

$$\frac{d(u_c)}{dt} = -\frac{u_c}{C.R} \quad (3)$$

$$\frac{d(i_1)}{dt} = \frac{U_1}{L_1} - \frac{R_1}{L_1} \cdot i_1 \quad (4)$$

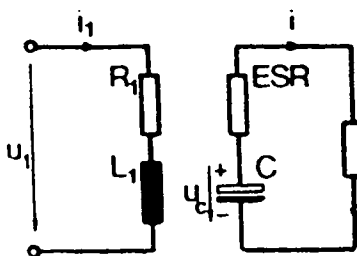
During the interval t_{off} the equivalent circuit of Fig 4b is applicable; the corresponding equations are

$$\frac{d(u_c)}{dt} = -\frac{u_c}{C.R} + \frac{N_1}{C.N_2} \cdot i_1 \quad (5)$$

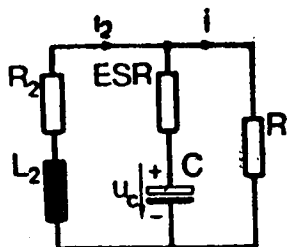
$$\frac{d(i_1)}{dt} = -\frac{N_2}{N_1} \cdot \frac{u_c}{L_2} - i_1 \cdot \frac{R_2}{L_2} \quad (6)$$

These two sets of equations, therefore, describe the system behaviour. Under the condition that the system time constants are large compared to the switching period we can combine these two sets of equations. The duty ratio shall be defined as

$$a = V_T = \frac{t_{on}}{T} \quad (7)$$



(a)



(b)

Fig 4 Equivalent circuits of the converter (U-R operation) (a) Turn-on switching state, and (b) Turn-off switching state

Weighted by this duty ratio, the combination of the two sets yields

$$\frac{d(u_c)}{dt} = -\frac{u_c}{C.R} + (1-a) \cdot \frac{N_1}{C.N_2} \cdot i_1 \quad (8)$$

$$\begin{aligned} \frac{d(i_1)}{dt} = & -(1-a) \cdot \frac{N_2}{N_1} \cdot \frac{u_c}{L_2} \\ & - i_1 \cdot \left[\frac{R_1}{L_1} \cdot a + (a-1) \cdot \frac{R_2}{L_2} \right] \\ & + a \cdot \frac{u_1}{N_1} \end{aligned} \quad (9)$$

The set of equations is transformed into a linearized system around the operating point by introducing

$$u_c = U_{c0} + \hat{u}_c$$

$$i_1 = I_{10} + \hat{i}_1 \quad (10)$$

$$a = a_0 + \hat{a}$$

$$\begin{bmatrix} \frac{d(\hat{u}_c)}{dt} \\ \frac{d(\hat{i}_1)}{dt} \end{bmatrix} = \begin{bmatrix} A_{11} & A_{12} \\ A_{21} & A_{22} \end{bmatrix} \cdot \begin{bmatrix} \hat{u}_c \\ \hat{i}_1 \end{bmatrix} + \begin{bmatrix} B_{11} \\ B_{21} \end{bmatrix} \cdot \hat{a} \quad (11)$$

with

$$\begin{aligned} A_{11} = & -\frac{1}{R_0 \cdot C}, & A_{12} = & (1-a_0) \cdot \frac{N_2}{C \cdot L_2 \cdot N_1}, \\ A_{21} = & -\frac{1-a_0}{L_2} \cdot \frac{N_2}{N_1}, \\ A_{22} = & -\left[a_0 \cdot \frac{R_1}{L_1} + (1-a_0) \cdot \frac{R_2}{L_2} \right], \\ B_{11} = & -\frac{I_{10} \cdot N_1}{C \cdot N_2}, & B_{21} = & \frac{U_{10}}{L_1} + \frac{U_{c0} \cdot N_2}{L_2 \cdot N_1} \\ & + \left[\frac{R_2}{L_2} - \frac{R_1}{L_1} \right] \cdot I_{10}. \end{aligned} \quad (12)$$

This leads to the structure diagram as shown in Fig 5.

The relationship for the stationary case results from

$$\frac{1}{C} \cdot \frac{N_1}{N_2} \cdot I_{10} \cdot (1-a) - \frac{U_{c0}}{R \cdot C} = 0 \quad (13)$$

$$\begin{aligned} \frac{R_2}{L_2} \cdot (a-1) \cdot I_{10} + \frac{N_2}{N_1 \cdot L_2} \cdot (a_0-1) \cdot U_{c0} \\ + (U_{10} + R_1 \cdot I_{10}) \cdot \frac{a_{10}}{L_1} = 0 \end{aligned} \quad (14)$$

In the operating point (given by U_{10} , U_{c0} , I_{10} and a_0)

Downloaded by [ETH Zurich] at 01:53 30 June 2015

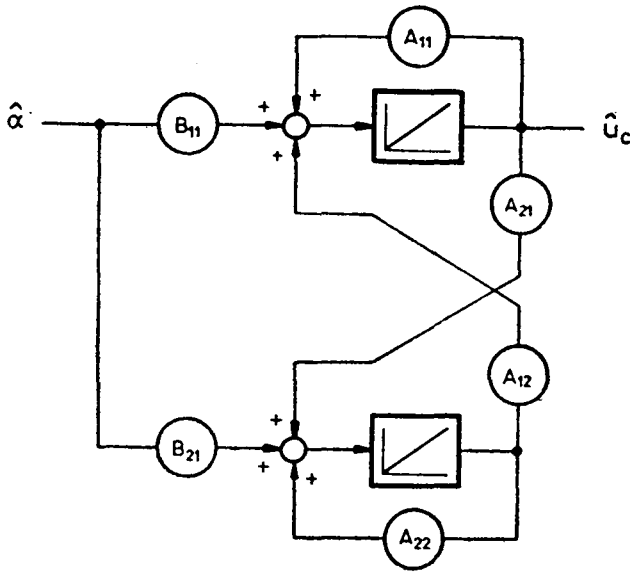


Fig 5 Structure diagram of the linearized bidirectional push-pull converter

we can calculate from (11) the transfer function between output voltage U_{c0} and the duty ratio α_0 .

We receive

$$u_c(s) = G_{u\alpha}(s) \cdot \alpha(s) \tag{15}$$

with

$$G_{u\alpha}(s) = \frac{s \cdot B_{11} + A_{12} \cdot B_{21} - A_{22} \cdot B_{11}}{s^2 - s \cdot (A_{11} + A_{22}) + \det(A)} \tag{16}$$

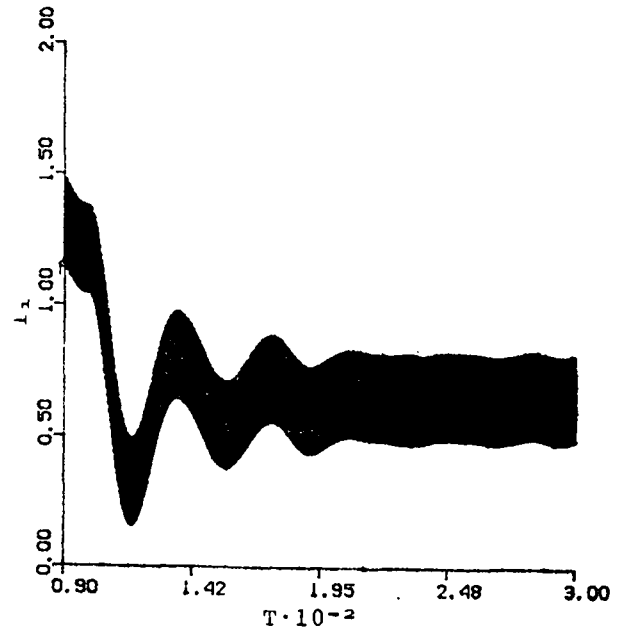
COMPARISON OF "AVERAGED" AND "SWITCHED" MODELS

For the models gained by averaging a weighting of the partial equation systems describing the instantaneously active system part is performed via the duty ratio, *ie*, via the operation time of the system. This method has been successfully applied for simulation and analysis of SMPS (Switched Mode Power Supplies) for many years (cf. [2]).

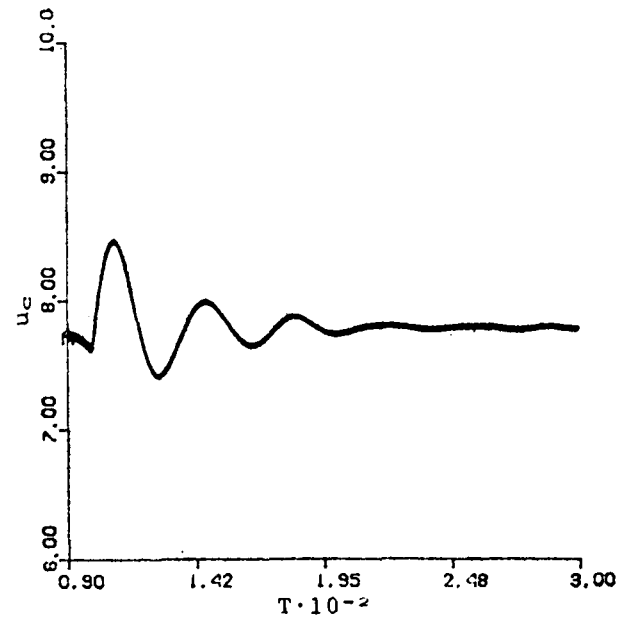
For the switched model one simulates, as the name implies, the switched system. One switches the system equations according to the switch positions. (The switches are assumed to be ideal). Furthermore, under certain conditions one can obtain theoretical models by using the z-transform. There exists ample literature [8].

For this paper the switched models have served as a means to vividly show the operational behaviour of the system and to obtain a means of checking the more simplified model gained by averaging.

Figure 6 illustrates the operation by showing the current in the transformer for a load step for the open system (*ie*, without closed-loop control). It also shows the related output voltage shape.



(a)



(b)

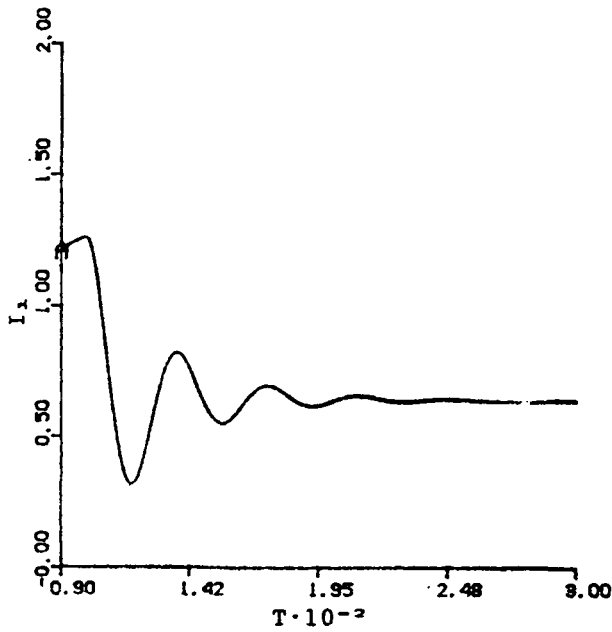
Fig 6 Load step for the uncontrolled bidirectional flyback-converter according to the switched model (a) Transformer current, and (b) Output voltage

For the simulation using the model gained by averaging we receive Fig 7. One can notice the good consistency of the results gained from both models. The substantially reduced calculation time for the "averaged" model has to be noted.

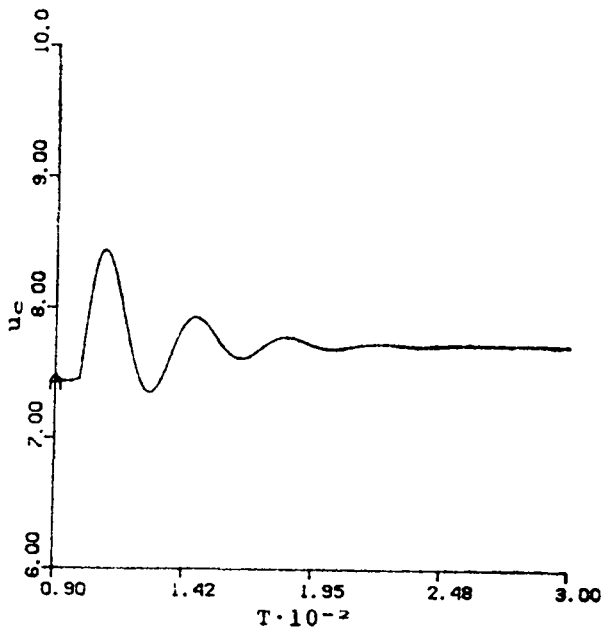
SINGLE-LOOP CONTROL

By linearization around the operating point the system of non-linear equations (8) and (9) has been transformed

Downloaded by [ETH Zurich] at 01:53 30 June 2015



(a)



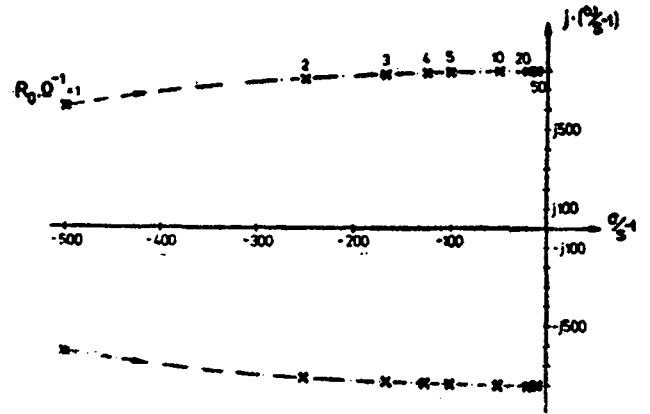
(b)

Fig 7 As Fig 6, but for the model gained from averaging

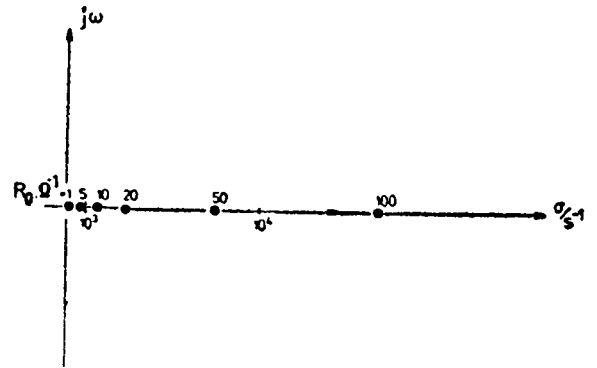
into a linear one (11). Therefore, it has been possible to give a transfer function of the bidirectional converter (16). Now it is possible to use the means of controller dimensioning for linear systems. One has to keep in mind, however, that the controller based on the dimensioning really works as designed only in the chosen operating point.

Pole zero diagram

In order to cover the operating behaviour for varying operating points one has to determine pole zero diagrams for a representative number of different operating points.



(a)



(b)

Fig 8 (a) Pole locations, (b) Zero locations for a bidirectional converter

Figure 8a shows the pole locations for a small experimental converter in dependency on the load. For lower load the poles come closer to the vertical axis and, therefore, the system becomes less damped. Figure 8b shows the locations of the zero for the same converter. The zero always lies in the right half plane and moves to the right for reduced load.

Bode plot of the controlled system

Figure 9 shows the Bode plot of the bidirectional converter. Now one can base the controller dimensioning on the Bode plot [4]. This results in a PI (proportional-integral) controller. One can show [3] that the controller gain is dependent very much on the converter load. On the other hand, the integration time constant remains almost constant. The Bode plot for the open control loop is shown in Fig 10. The controller has to be dimensioned for the worst case. Here, this would be for the least damping of the controlled system.

Bode plot of the closed loop

The Bode plot (Fig 11) shows the closed loop system behaviour for reference value changes. However, for application as converter for constant output voltages the

Downloaded by [ETH Zurich] at 01:53 30 June 2015

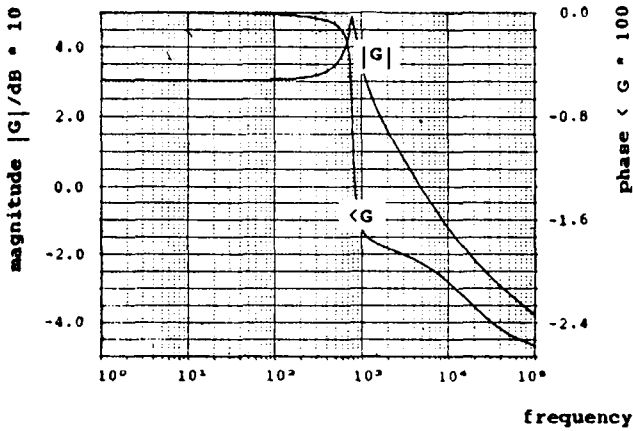


Fig 9 Bode plot of the converter

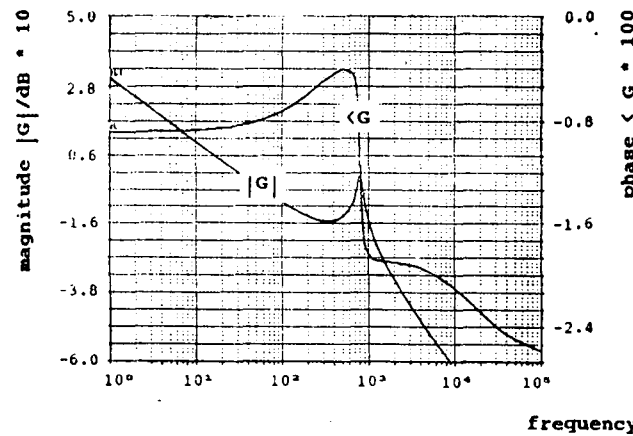


Fig 10 Bode plot for the open control loop

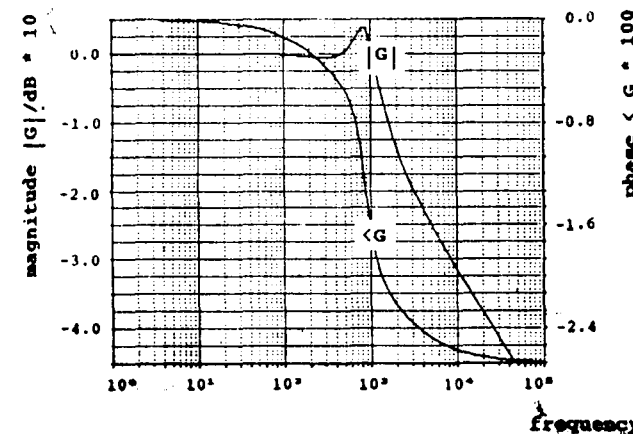


Fig 11 Bode plot for the closed loop

behaviour relative to load changes (disturbance frequency response) is decisive.

System step response

The research in [3] has shown that the control quality of a single loop voltage control cannot meet higher standards. Damping of the system basically is given by the

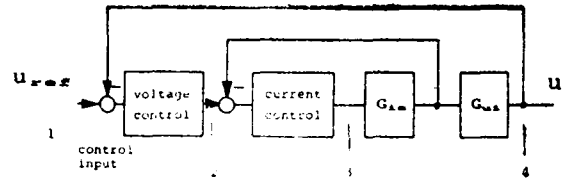


Fig 12 Cascade control structure

load. Stability considerations have shown very unfavourable positions of the system poles and zeros. The controller such dimensioned is only applicable for a limited operating region.

THE BIDIRECTIONAL CONVERTER WITH CASCADE CONTROL

Partial transfer functions

Dividing the overall transfer function (16) into two partial transfer functions ($G_{u_i}(s) = G_{i_x}(s) \cdot G_{u_i}(s)$) makes it possible to design a two loop control structure (Fig 12). There $G_{i_x}(s)$ represents the relationship between the duty ratio and the converter current and $G_{u_i}(s)$ gives the relationship between converter current and output voltage.

The state vector representation is

$$\dot{x} = A x + B u \tag{17a}$$

$$y = C \cdot x + D \cdot u \tag{17b}$$

where equation (17a) is defined by (11) where matrix B is a vector b; in (17b) matrix C is reduced to a vector c and matrix D is reduced to a scalar.

Now we can (according to [4]) determine the transfer function as

$$G(s) = c^T \cdot (s \cdot I - A)^{-1} \cdot b + d \tag{18}$$

For the determination of the transfer function G_{i_x} (which gives the relationship between converter current i_1 and the duty ratio a), we have $c^T = (0,1)$ and $d = 0$ (17b) - the output equation - is reduced to $y = i_1$). This results in (for $\det A$ cf. (22))

$$G_{i_x}(s) = \frac{s \cdot B_{21} + A_{21} \cdot B_{11} - A_{22} \cdot B_{11}}{s^2 - s \cdot (A_{11} + A_{22}) + \det A} \tag{19}$$

The relationship between output voltage u_c and converter current i_1 is given by

$$G_{u_i}(s) = \frac{s \cdot B_{11} + A_{12} \cdot B_{21} - A_{22} \cdot B_{11}}{s \cdot B_{21} + A_{21} \cdot B_{11} - A_{11} \cdot B_{21}} \tag{20}$$

The overall transfer function of the converter system now has been split into two partial transfer functions (Fig 13). Now one can design a controller for the current control section and thereby stabilize the inner loop. The

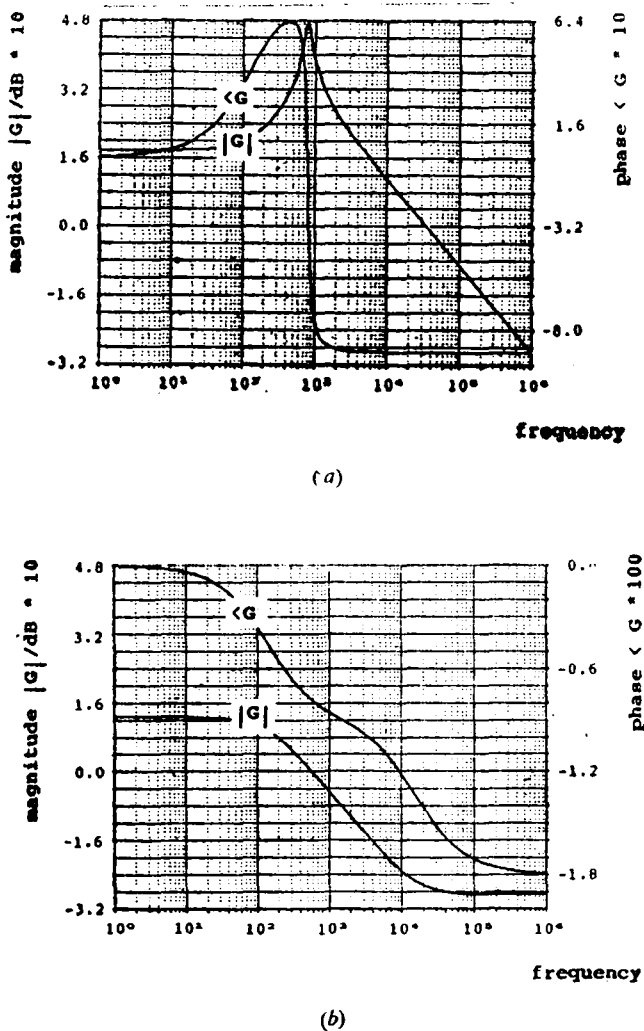


Fig 13 Bode diagrams for the partial transfer functions (a) $G_{ia}(s)$, and (b) G_{ii}

transfer function resulting from this now together with the relationship between converter current and output voltage $G_{ui}(s)$ (20) represents the section to be controlled by the voltage controller. The voltage controller now can be designed separately. Now, for the design we can apply all means for the control design for linear systems [4]. For the application of cascade control for conventional SMPS there exist numerous references [7].

Inner control loop - Inner loop current controller

Design of the P (proportional) - controller

The transfer function (between points 2 and 3 in Fig 12) of the current control loop results in

$$G_{iP}(s) = K_P \cdot \frac{B_{21} \cdot s + A_{21} \cdot B_{11} - A_{11} \cdot B_{21}}{s^2 + s \cdot (-A_{11} - A_{22} + K_P \cdot B_{21}) + \det A + K_P \cdot bc} \quad (21)$$

$$\text{with } \det A = A_{11} \cdot A_{22} - A_{21} \cdot A_{12} \quad (22)$$

$$bc = A_{12} \cdot B_{21} - A_{22} \cdot B_{11}$$

and K_P as the gain of the P - controller.

As shown in [5] it is not necessary to use PI - control or higher order control for the inner loop.

The outer control loop—the voltage control

In a second step now an outer loop voltage control will be designed. Dependent on the current control realization we receive different systems to be controlled for the voltage controller.

The transfer function (between points 2 and 4 in Fig 12) of the controlled system for voltage control with inner loop P current control circuit is

$$G_u(s) = K_P \cdot \frac{B_{11} \cdot s + A_{12} \cdot B_{21} - A_{22} \cdot B_{11}}{s^2 + s \cdot (-A_{11} - A_{22} + K_P \cdot B_{21}) + \det A + K_P \cdot ab} \quad (23)$$

$$ab = A_{21} \cdot B_{11} - A_{11} \cdot B_{21}$$

As shown in [5], a PI - control for the outer loop is sufficient. The transfer function for a PI - controller is

$$G_{uPI}(s) = \frac{K_{Iu} \cdot (1 + s \cdot T_{Iu})}{s \cdot T_{Iu}} \quad (24)$$

Transfer function for the overall system

For the overall system the following transfer function (between points 1 and 4 in Fig 12) results for a PI - voltage controller with P - current controller

$$G(s) = \frac{\delta_2 \cdot s^2 + \delta_1 \cdot s + \delta_0}{\mu_3 \cdot s^3 + \mu_2 \cdot s^2 + \mu_1 \cdot s + \mu_0} \quad (25)$$

$$\text{with } \delta_2 = K_{Iu} \cdot K_{Ii} \cdot B_{11} \cdot T_{Iu}$$

$$\delta_1 = K_{Iu} \cdot K_{Ii} \cdot (B_{11} + T_{Iu} \cdot bc)$$

$$\delta_0 = K_{Iu} \cdot K_{Ii} \cdot bc$$

$$\mu_3 = T_{Iu} \quad (26)$$

$$\mu_2 = T_{Iu} \cdot (-A_{11} - A_{22} + K_P \cdot B_{21}) + K_{Iu} \cdot K_{Ii} \cdot B_{11} \cdot T_{Iu}$$

$$\mu_1 = T_{Iu} \cdot (\det A + K_P \cdot ab) + K_{Iu} \cdot K_{Ii} \cdot (B_{11} + T_{Iu} \cdot bc)$$

$$\mu_0 = K_{Iu} \cdot K_{Ii} \cdot bc.$$

The controller design was performed with the means of the classical linear control theory. For the practical design we have to consider the limitations of the duty ratio and of maximum permissible transformer (converter) current, however, the controller parameters therefore have to be checked for their validity.

STATE SPACE CONTROLLER

Simple state space controller

Another possibility to obtain a good closed loop response is to realize a state space controller. An exami-

nation of the simple state space control structure (Fig 14) shows that this structure only has limited applicability to the control of the bidirectional converter. The prefilter can only be dimensioned exactly if the knowledge of the system is very good. However, the nonlinearity of the system leads to a prefilter which can successfully be applied only in a small region around the operating point. A small deviation from the operating point leads to an undesired stationary control error. Therefore, a fourth concept is investigated in next section.

Extended state space control

Taking the control error as another state variable [6] we receive an extended state space control structure (Fig 15). This leads to very satisfactory operating conditions.

Starting with the system equation (11) one can determine the elements of the controller matrix according to [6]. There the pole locations are chosen

$$\begin{aligned} s_1 &= \sigma_1 + j\Omega \\ s_2 &= \sigma_1 + j\Omega \\ s_3 &= \sigma_2 \end{aligned} \tag{27}$$

with $\sigma_1, \sigma_2 < 0$.

A rather lengthy calculation leads to the elements of the controller, described by a (1×3) matrix here. (The practical realization of the controller only requires an adder circuit with an operational amplifier—the real practical problem here as well as for the cascade control lies in the exact and disturbance free measurement of i_1).

$$\begin{aligned} r_{12} &= \frac{[m_2 + \sigma^2 + \Omega^2 + 2 \cdot \sigma_1 \cdot \sigma_2 + q_{23}/q_{33} \cdot (\sigma_1^2 \cdot \sigma_2 + \Omega^2 \cdot \sigma_2)] \cdot q_{11} - [m_1 - 2 \cdot \sigma_1 - \sigma_2] \cdot q_{21}}{q_{11} \cdot q_{22} - q_{21} \cdot q_{12}} \\ r_{11} &= \frac{[m_1 - 2 \cdot \sigma_1 - \sigma_2] \cdot q_{22} - [m_2 + \sigma^2 + \Omega^2 + 2 \cdot \sigma_1 \cdot \sigma_2 + q_{23}/q_{33} \cdot (\sigma_1^2 \cdot \sigma_2 + \Omega^2 \cdot \sigma_2)] \cdot q_{12}}{q_{11} \cdot q_{22} - q_{21} \cdot q_{12}} \\ r_{13} &= \frac{(\sigma_1^2 \cdot \sigma_2 + \Omega^2 \cdot \sigma_2)}{q_{33}} \end{aligned} \tag{28}$$

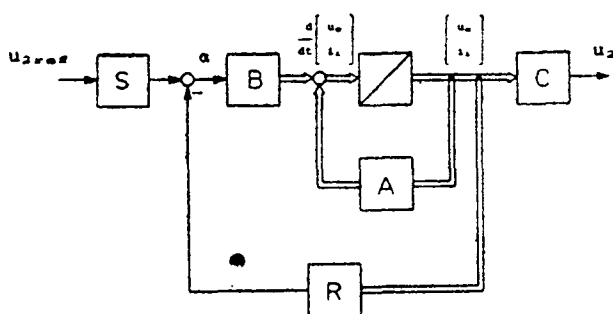


Fig 14 Simple state space control structure (for A, B see (17a)), R ..controller matrix, C becomes $c^T = (1,0)$

with the abbreviations

$$\begin{aligned} q_{11} &= B_{11}, & q_{12} &= B_{21} \\ q_{21} &= -A_{22} \cdot B_{11} - B_{21} \cdot A_{12} \\ q_{22} &= -A_{11} \cdot B_{21} + A_{21} \cdot B_{11} \\ q_{23} &= -B_{11} \cdot q_{33} = -A_{12} \cdot B_{21} + A_{22} \cdot B_{11} \\ m_1 &= A_{11} + A_{22} \\ m_2 &= -A_{11} \cdot A_{22} + A_{21} \cdot A_{12} \end{aligned} \tag{29}$$

System step response

The advantage of the state space approach (Fig 16) is that the system behaviour can be chosen to a large extent by selection of the pole positions (27). One has to keep in mind, however, that *eg* the values of σ and Ω have to be selected such that the limitations of the state and controller variables are not reached. Such limitations are, *eg*, given by the maximum transistor currents, by core saturation and by the fact that $a < 0$ and $a > 1$ could result from the controller calculation but are not physically realizable, etc.

APPLICATIONS

Uninterruptible power supplies

Uninterruptible power supplies (UPS) are indispensable today for many applications in industry, medicine and data processing.

Uninterruptible DC voltage

In systems which use a DC bus bar by which the different users are supplied (either directly or via a DC-DC converter) the application of a bidirectional flyback converter as battery charging device or as a DC transformer between battery and DC bus bar can be performed either by rectification from a mains by AC/DC conversion or by a DC voltage source. The converter is connected to the voltage DC link and adjusts the battery voltage to the DC link voltage by appropriate selection of the transformation

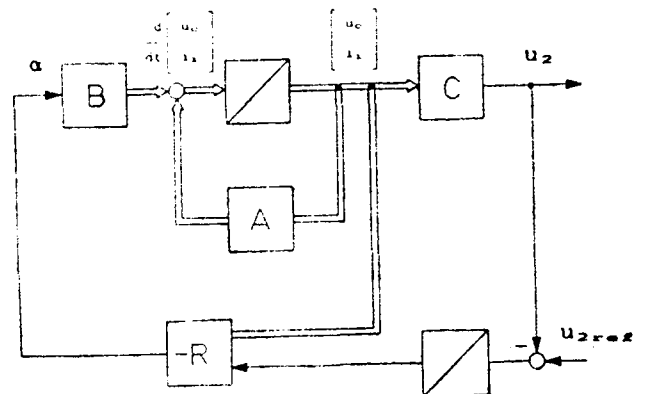


Fig 15 Extended state space control structure (for A, B, C, R see Fig 14)

Downloaded by [ETH Zurich] at 01:53 30 June 2015

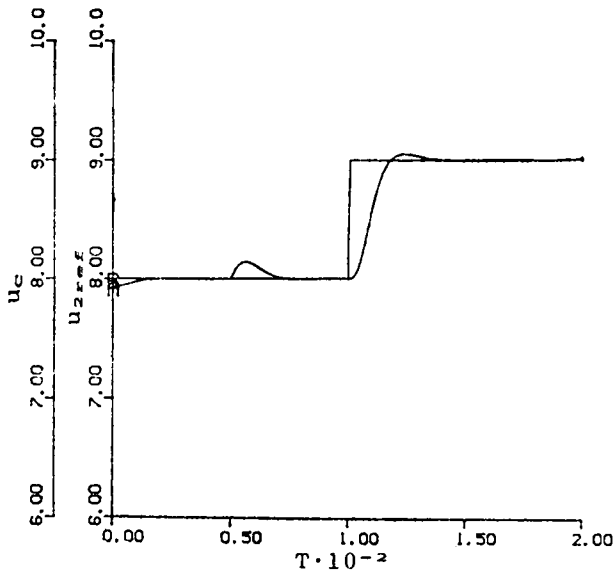


Fig 16 System step response to load change at T_1 and reference value change at T_2

ratio. The relationship between battery voltage U_B and DC voltage U_Z of the DC link is given by

$$U_B = \frac{N_2}{N_1} \cdot \frac{a}{a-1} \cdot U_Z \quad (29)$$

The system architecture is especially advantageous for isolated systems which are, eg, supplied by solar cells. One example are distributed measurement stations which have to work completely independently of public supply mains. The bidirectional flyback converter serves as battery charging unit in this application, or, if the DC bus bar supply is omitted, as new supply source. Especially for solar systems also mixed operation can be advantageous (ie, energy is supplied from the solar cells while additionally power flow from the storage battery exists).

Operation as classical SMPS

As a closer analysis shows [10], especially for trapezoidal (continuous) operation a loss reduction on the secondary side by replacement of the diode by a switching device with ohmic forward characteristic can be achieved.

A further improvement of the efficiency is possible by extension of the circuit operation to quasi-resonant operation [11]. The good dynamical behaviour achievable by the operation which can be defined as quasi-triangular operation is treated in detail in [10].

CONCLUSION

This paper has shown the system behaviour analysis and the controller design for a bidirectional buck-boost converter. Dimensioning guidelines have been given for

controller structures with one-loop control, with two-loop (cascade) control and for state space control. The system behaviour has been investigated for all these cases. It has been shown that the one-loop control does not yield satisfactory results. The cascade control and the state space control, however, lead to very good control behaviour. This concerns the stability, as well as the dynamic quality (such as fast control response).

Due to a clearer treatment and for the sake of brevity the investigations have been constrained to a resulting energy flow (averaged over one pulse period) from the primary to the secondary side. For reverse power flow (ie, from the secondary to the primary) and control of the secondary voltage there do not exist a right-half plane zero of the transfer function of the open system. This substantially simplifies the task of stabilization. Therefore, a closer discussion shall be omitted here, but can be found in [10].

ACKNOWLEDGEMENT

The authors are very much indebted to the Austrian Fonds zur Förderung der wissenschaftlichen Forschung, who supports the work of the power electronics section at their university.

REFERENCES

1. J W Kolar, F A Himmelstoss & F C Zach, Analysis of the control behaviour of a bidirectional high-frequency DC-DC-converter, *Proc PCIM'88*, München, pp 344-359, May 1988.
2. R D Middlebrook & S Cuk, *Advances in switched-mode power conversion*, Pasadena, Teslaco, vol 1, 1981.
3. F A Himmelstoss, J W Kolar & F C Zach, Analysis of closed-loop control behaviour of a bidirectional high frequency DC-DC converter, *Proc PCIM'88*, pp 174-184, Tokyo, Dec 1988.
4. O Föllinger, *Regelungstechnik*, Hüthig Verlag, Heidelberg, 1984.
5. F A Himmelstoss, J W Kolar & F C Zach, Analysis of the cascade control behaviour of a bidirectional high frequency DC-DC converter, *Proc HFPC'89*, Naples Fl., May 1989.
6. A Weinmann, *Regelungstechnik*, Springer, Wien, vol 3, 1986.
7. T Kawabata *et al*, Chargerless UPS using multifunctional BIMOS inverter, *IEEE IAS Annual Meeting*, pp 513-520, 1986.
8. G Eggers, New power system modelling approaches on the basis of equivalent state variables, *Proc European Space Power Conf*, Madrid, pp 61-70, Oct 1989.
9. F A Himmelstoss, J W Kolar & F C Zach, Comparison of control structures for a bidirectional high-frequency DC-DC converter, *Proc European Space Power Conf*, Madrid, pp 403-408, Oct 1989.
10. F A Himmelstoss, Der bidirektionale Sperrwandler im kontinuierlichen Betrieb, *PhD thesis*, TU Vienna, 1990.
11. J W Kolar, F A Himmelstoss & F C Zach, Analysis and comparison of a unidirectional and a bidirectional quasiresonant converter, *Proc PCIM'90*, Munich, June 1990.